Environmental and Experimental Botany 169 (2020) 103904

Contents lists available at ScienceDirect

Environmental and Experimental Botany

journal homepage: www.elsevier.com/locate/envexpbot

Embryo responses to extreme water events provide insights into the behavior of *Butia capitata* (Arecaceae) seed banks during hydration cycles

Bruno Guilherme Gonçalves[a], Leonardo Monteiro Ribeiro[b,*], Daiane Souza Dias[b], Hellen Cássia Mazzottini-dos-Santos[b], Cristina de Paula Santos Martins[a], Paulo Sérgio Nascimento Lopes[a], Maria Olívia Mercadante-Simões[b]

[a] Instituto de Ciências Agrárias, Universidade Federal de Minas Gerais, 39404-547, Montes Claros, Minas Gerais, Brazil
[b] Departamento de Biologia Geral, Universidade Estadual de Montes Claros, 39401-089, Montes Claros, Minas Gerais, Brazil

ARTICLE INFO

Keywords:
Arecaceae
ABA
Fast hydration
Oxidative stress
Water stress

ABSTRACT

Dormant seed embryos in seed banks can experience hydration cycles that subject them to water stress (WS) and then fast hydration (FH). Physiological and cytological aspects of embryos of the Cerrado (neotropical savanna) palm *Butia capitata* were evaluated when subjected to osmotically induced WS and FH. The water potential (ψ_w), viability, and vigor of dehydrated or hydrated embryos were determined after immersion in osmotic solutions. Embryos were submitted to FH (ψ_w = 0 MPa), moderate WS (ψ_w = −1 and −2 MPa), and severe WS (ψ_w = −2 and −4 MPa). Indicators of oxidative stress (H_2O_2, O_2^-, MDA, and CAT, SOD, and APX activities), membrane functionality (electrical conductivity and leaching of K^+, Mg^{2+}, and Ca^{2+}), and ABA content were evaluated. The ultrastructures of dehydrated embryos and hydrated embryos submitted to ψ_w = 0, −1, and −2 MPa were evaluated. Dehydrated embryos (ψ_w = −8.5 MPa) showed high tolerance to WS that was related to their abundant protein reserves, SOD activities, and high ABA contents. Embryos tolerate FH and hydration makes ψ_w = −0.2 MPa. Hydrated embryos also show high tolerance to WS, which is related to their control of oxidative stress and increases in their ABA contents. Loss of viability under severe WS occurs associated with the blockage of protein mobilization, loss of membrane functionality, and the collapse of cellular structure. Embryo tolerance to WS and FH is crucial to the resilience of *B. capitata* seed banks exposed to hydration cycles in the seasonal Cerrado biome environment.

1. Introduction

Many plants growing in environments with seasonal climates produce seeds with germination-blocking mechanisms (i.e., dormant seeds) (Bewley et al., 2013; Baskin and Baskin, 2014). Those seeds are commonly buried in the soil, and compose a component of the species population known as the seed bank (Long et al., 2014). The seeds in the seed bank can experience several cycles of hydration, alternating between states of hydration and dehydration until dormancy is overcome (Bewley et al., 2013).

Hydration cycles are important signaling mechanisms for overcoming dormancy but expose embryonic cells to stressful, and potentially fatal, conditions (El-Maarouf-Bouteau and Bailly, 2008; Baskin and Baskin, 2014). Water stress (WS) in seed banks may result from prolonged periods of drought followed by fast hydration (FH) as a consequence of intense seasonal rainfall. Both WS and FH can damage cell membranes, and WS is also associated with oxidative stress due to imbalances between reactive oxygen species (ROS) production and removal that can result in membrane, protein, and DNA damage (Apel and Hirt, 2004; Bailly, 2004; Berjak and Pammenter, 2008; Bewley et al., 2013). The modulation of oxidative stress through enzymatic (SOD, CAT, APX, and GPX activity) and non-enzymatic (vitamin E, flavonoids, among others) mechanisms can prevent cell damage and allow the use of ROS as signaling agents in various metabolic processes (Bailly, 2004). ABA is a phytohormone associated with the maintenance of seed dormancy, and its synthesis and degradation pathways are influenced by oxidative stress, but may induce increased antioxidant system efficiency (Ozfidan et al., 2012; Souza et al., 2017). Our knowledge concerning the metabolic and ultrastructural responses to WS is still quite restricted in terms of tropical species, and additional studies are needed – especially those focusing on uncultivated species (Bewley et al., 2013; Huang and Song, 2013).

Abbreviations: ABA, abscisic acid; APX, ascorbate peroxidase; CAT, catalase; GPX, glutathione peroxidase; SOD, superoxide dismutase; ψ_w, water potential

* Corresponding author.
E-mail address: leonardo.ribeiro@unimontes.br (L.M. Ribeiro).

https://doi.org/10.1016/j.envexpbot.2019.103904
Received 25 June 2019; Received in revised form 30 September 2019; Accepted 7 October 2019
Available online 14 October 2019

Butia capitata (Mart.) Becc. is an endemic palm tree of the Cerrado (neotropical savanna) biome in central Brazil that has significant ecological and economic importance, although threatened by deforestation and agricultural development (Magalhães et al., 2013; Oliveira et al., 2013). The seeds of the species show pronounced dormancy, and its seed banks are subject to WS during long periods of seasonal drought, which can be amplified by fires common to Cerrado environments (Carvalho et al., 2015; Dias et al., 2017; Mazzottini-dos-Santos et al., 2018). *B. capitata* seeds exhibit intermediate (between orthodox and recalcitrant) behavior (Dias et al., 2015) – a still poorly studied pattern characterized by desiccation tolerance but low temperature intolerance (Marques et al., 2018).

The objective of the present study was to evaluate the physiological (water potential, oxidative stress, and membrane functionality) and ultrastructural aspects of *B. capitata* embryo responses to osmotically induced WS. We addressed the following questions: i) what are the physiological responses of dehydrated and hydrated embryos to WS? ii) What are the effects of hydration on embryo physiology and ultrastructure? We also sought to examine ecophysiological aspects related to WS tolerance, and its implications for seed bank maintenance in natural environments.

2. Methods

2.1. Collection and storage of plant material

We collected ripe fruits of *Butia capitata* (identifiable by the yellowish color of their epicarps and the easy abscission of the bunch) in natural populations located in northern Minas Gerais State, Brazil, in the municipalities of Mirabela (16°26′64″S; 44°19′34″W), during the 2017/2018 harvest, and in Bonito de Minas (15°25′59.8″S; 44°41′31.7″W) and Itacambira (17°03′54″S; 43°18′32″W), during the 2018/2019 harvest. The fruits were mechanically depulped and the pyrenes (seeds enveloped by the woody endocarp) kept in a shaded and ventilated storage site for up to 60 days (after which the experiments were initiated). Each experiment was carried out with seeds from the same batch.

2.2. Water relations

We evaluated the WS response of isolated embryos from dehydrated or hydrated seeds. Dehydrated seeds were obtained from pyrenes stored in the shade at room temperature for between 30 and 60 days after endocarp rupture (using a manual vise). Hydrated seeds were obtained by immersing isolated seeds in distilled water for 72 h at 25 °C, when the start of phase II of germination (Bewley et al., 2013) was reached (Oliveira et al., 2013). We determined the water contents of the dehydrated or hydrated seeds and their embryos (extracted using scalpels) by comparing their fresh and dry masses, after dehydration at 105 °C for 24 h (Brasil, 2009), using five replicates of 10 seeds or embryos.

We determined the water potentials (ψ_w) of isolated embryos obtained from dehydrated or hydrated seeds (hereinafter called respectively dehydrated embryos and hydrated embryos) by immersing them in solutions of polyethylene glycol 6000 (PEG 6000 - an inert and non-toxic osmotic agent that does not penetrate cell membranes; Michel and Kaufmann, 1973) to simulate stressful conditions that affect the water capacities of embryos – defined here as their ability to absorb or retain water. As dehydrated embryos already have low ψ_w values, more negative potentials were applied to them than used for hydrated embryos. Thus, PEG 6000 concentrations were used that provided $\psi_w = 0$, -2, -4, -6, -8 and -10 MPa (applied to dehydrated embryos) and $\psi_w = 0$, -0.5, -1, -2, -3 and -4 MPa (applied to hydrated embryos). Preliminary tests indicated that the most negative ψ_w used would alter the water capacity (capacity of the dehydrated embryos to absorb water, and the capacity of the hydrated embryos to retain water) between 1.5 and 2 times in relation to the $\psi_w = 0$ obtained with distilled water. We calculated PEG 6000 concentrations using the equation of Michel and Kaufmann (1973), considering 25 °C, as the reference temperature. The fresh masses of the embryos were determined in their initial condition, and after 12, 24 and 36 h of immersion in the osmotic solutions (using five replicates of ten embryos each) and their water contents variations were calculated. The ψ_w was calculated for each immersion time based on the adjustments of quadratic equations, considering that $\psi_{w\text{-embryo}} = \psi_{w\text{-solution}}$, when water flow is zero. The viability and vigor of dehydrated and hydrated embryos when submitted to different ψ_w for 12 h were evaluated using the tetrazolium test, following the criteria established by Ribeiro et al. (2010).

In order to carry out the physiological evaluations presented below, we selected $\psi_w = 0$ and ψ_{ws} values that simulated moderate stress (reduction of water capacity, but the maintenance of viability and reduction of vigor), and severe stress (loss of viability in more than 60% of the embryos) for both dehydrated embryos and hydrated embryos, based on evaluations of embryo mass variations, viability, and vigor. The ψ_{ws} that provided moderate and severe water stress were: -2 and -4 MPa for dehydrated embryos, and -1 and -2 MPa for hydrated embryos.

2.3. Histolocalization of superoxide ions (O_2^-)

We performed histolocalization of O_2^- in the apoplast according to Oracz et al. (2012), with modifications (Bicalho et al., 2019). Twenty embryos from each treatment were immersed in 500 µL of nitroblue tetrazolium (1 mM) in Tris-HCl buffer (10 mM, pH 7.0) and kept at room temperature for 10 min. The embryos were washed three times in Tris-HCl buffer (10 mM, pH 7.0), and their images captured using a digital camera coupled to a stereomicroscope.

2.4. Hydrogen peroxide (H_2O_2) quantification

We macerated four replicates of 30 mg of embryos from each treatment in liquid nitrogen (using a mortar and pestle). The material and 400 µL of 0.1% TCA (m/v) was added in 2 mL Eppendorf tubes; the extract was then vortexed for 1 min and centrifuged at 10,000 × *g* for 15 min at 4 °C. We removed a 250 µL aliquot of the supernatant and added it to 250 µL of 100 mM potassium phosphate buffer (pH 7.5) and 1000 µL of 1 M potassium iodide. The tubes with the solutions were placed on ice in the absence of light for one hour; the samples were then held in the dark at room temperature for 20 min to stabilize the reaction. We subsequently analyzed the samples in a spectrophotometer (UV-1800, Shimadzu, Tokyo, Japan) at 390 nm, and the amount of H_2O_2 was expressed in µmol g^{-1} dry mass based on a pre-established standard curve (Alexieva et al., 2001).

2.5. Evaluation of the enzymatic activities of the antioxidant system

We macerated four replicates of 20 mg of embryos from each treatment in liquid nitrogen. Samples were vortexed for 1 min in PVPP (10% w/v), 500 µL of sodium phosphate buffer (50 mM, pH 6.8), 10 µL of EDTA (100 µM), and 490 µL of deionized water, and the extracts centrifuged at 10,000 × *g* at 4 °C for 15 min. SOD, CAT, and APX activities were determined in 100 µL of supernatant.

We determined SOD activity by adding the extract to a solution containing methionine (13 mM), NBT (75 µM), 100 µM riboflavin EDTA (2 µM), and potassium phosphate buffer (50 mM, pH 7.8). The solutions were then illuminated by fluorescent lights (15 W) at 25 °C. After 10 min of light exposure, enzyme activity was terminated with the interruption of light. Control reactions were kept in the dark for 10 min. We analyzed the blue formazan compound by spectrophotometry (UV-1800, Shimadzu, Tokyo, Japan) at 575 nm, defining a SOD unit as the amount of enzyme required to inhibit 50% of NBT photoreduction. The results are presented in U min^{-1} g^{-1} protein (Giannopolitis and Ries,

1977).

For CAT activity determinations, we added the extract to potassium phosphate buffer (50 mM, pH 7.0) and H_2O_2 (12.5 mM) freshly prepared at the time of analysis. The analyses were performed in a spectrophotometer at 240 nm for 1 min. CAT activity was estimated using a molar extinction coefficient (ε) equal to 39.4 $mM^{-1}\,cm^{-1}$ (Cakmak and Horst, 1991); the results are expressed in mmol of H_2O_2 $minute^{-1}\,g^{-1}$ protein.

We examined APX activity by adding the extract to potassium phosphate buffer (50 mM, pH 6.8) and, at the time of analysis, ascorbate (0.25 mM) and H_2O_2 (1.0 mM). The oxidation rate of ascorbic acid was monitored for 1 min, recording absorbance values at 290 nm every 10 s in a spectrophotometer. We determined APX activity using ε equal to 2.8 $mM^{-1}\,cm^{-1}$, expressing the results in μmol of ascorbate $minute^{-1}\,g^{-1}$ protein (Nakano and Asada, 1981).

2.6. Malondialdehyde (MDA) quantification

We macerated four replicates of 30 mg of embryos from each treatment in liquid nitrogen, and then added 1.5 mL of trichloroacetic acid (TCA) 0.1% (w/v). After vortex homogenization for 1 min, the samples were centrifuged at 12,000 x g for 15 min. A 1 mL aliquot of the supernatant was withdrawn and 3 mL of a 0.5% (m/v) thiobarbituric acid solution (prepared in 20% TCA) was added. The solution was then held for 60 min at 95 °C and subsequently cooled on ice for 10 min. We analyzed the samples spectrophotometrically (UV-1800, Shimadzu, Tokyo, Japan) at wavelengths of 532 and 660 nm, eliminating interferences by subtracting the values obtained at wavelengths (532–660). MDA concentrations are expressed as nmol g^{-1} dry mass (Heath and Packer, 1968, adapted).

2.7. ABA quantification

We quantified ABA by means of high performance liquid chromatography (HPLC), macerating the samples in liquid nitrogen in 2 ml Eppendorf tubes (using four replicates of 100 mg of embryos from each treatment). We then added 1 mL of an extraction solvent (methanol, isopropanol, and acetic acid in proportions of 20: 79: 1) to each sample. The solutions were vortexed for 1 min, submitted to ultrasonic disassociation (Quimis, 0335D, Diadema, Brazil) for 30 min (water temperature of 4–7 °C) and again vortexed for 1 min. The solution obtained was centrifuged for 15 min at 4 °C and 10,000 x g. We collected the supernatant and 0.5 mL of the extraction solvent was added to the precipitate and the extraction procedure repeated two more times. The supernatants collected from each extraction were mixed, homogenized, and then filtered (0.22 μm porosity filter). The filtrate was injected into the chromatographic system under the following conditions: 20 μl of sample in a HPLC system coupled to a diode array detector (1290 Infinity, Agilent Technologies, Waldbronn, Germany), with a flow rate of 0.8 ml $minute^{-1}$, column temperature 30 °C, with methanol as the mobile phase (Müller and Munné-Bosch, 2011, adapted); detection used the wavelength of 250 nm. We identified the ABA chromatographic peaks in the samples by comparing their retention times with that of an analytical standard. The results are expressed in ng g^{-1} dry mass.

2.8. Estimating membrane functionality - solute leaching

We immersed four replicates of 20 embryos from each treatment (whose masses had been determined) in ultrapure water for 4 h and held them in a germination chamber at 30 °C. The electrical conductivities of the solutions were analyzed using a conductivity meter (AKSO, AK83, São Leopoldo, Brazil). We quantified the K^+, Mg^{2+} and Ca^{2+} ions in the solutions using an atomic absorption spectrophotometer (AA 240, Varian, Santa Clara, USA), according to a methodology adapted from Gomes-Copeland et al. (2012). The results are expressed on a dry mass basis.

2.9. Ultrastructural and cytochemical evaluations

Transmission electron microscopic analyses were made of the cotyledonary petioles of *B. capitata* from dehydrated embryos (control) and hydrated embryos submitted to ψ_w = 0, -1 and -2 MPa. Samples were fixed in Karnovsky's solution (Karnovsky, 1965), with post-fixation in 1% osmium tetroxide, in 0.1 M phosphate buffer, pH 7.2 (Roland, 1978). The ultrafine sections of the peripheral region of the cotyledonary petiole (including protoderm and ground meristem cells) were contrasted with uranyl acetate (Watson, 1958) and lead citrate (Reynolds, 1963) and examined by transmission electron microscopy (Philips/FEI Company, Eindhoven, Netherlands) at 80 kV.

In order to identify embryonic reserves, we prepared additional samples of the same materials used for the ultrastructural evaluations. The material was fixed in Karnovsky's solution (Karnovsky, 1965), dehydrated in ethylic series and included in (2-hydroxyethyl)-methacrylate (Leica Microsystems, Heidelberg, Germany). Longitudinal sections (5 μm thick) were obtained using a rotary microtome (Atago, Tokyo, Japan) and stained with Xylidine-Ponceau (Vidal, 1970) for proteins; periodic acid and Schiff reagent - PAS (Feder and O'Brien, 1968) for neutral polysaccharides; and Sudan black in glycerin 10% (Johansen, 1940, modified) for lipids.

2.10. Statistical analysis

The quantitative data of viability, vigor, H_2O_2, SOD, MDA, ABA, electrical conductivity, and leaching of K^+ and Mg^{2+} were submitted to analysis of variance, and their means compared by the Tukey test, at a 5% level of probability. Data on Mg leaching were arcsine transformed $(x100^{-1})^{-2}$ for the comparisons.

3. Results

3.1. Water relations

Dehydrated seeds of *B. capitata* and their embryos presented, in their initial (fresh) conditions, water contents of 5.4 and 9.9%, respectively. Immersion in distilled water for 72 h increased their water contents to 25.6% in the seeds and to 64.8% in the embryos; the dry masses of the hydrated or dehydrated embryos did not differ (Fig. 1A). Hydration increased the water contents (dry conditions) of the seeds and their embryos by 5.6 and 17.7 times respectively (Fig. 1B).

The dehydrated embryos (0.11 g H_2O g^{-1} DM) showed increases of approximately two-fold in their water contents when submitted to

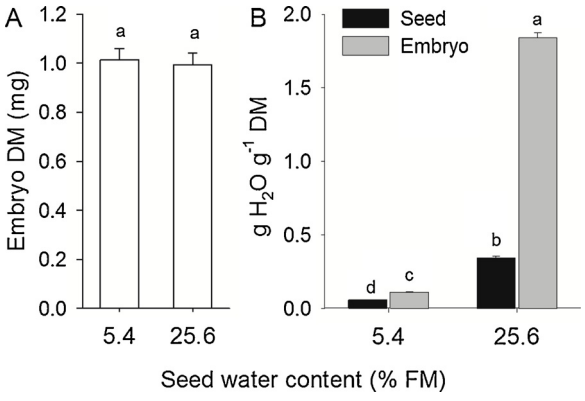

Fig. 1. Dry masses of *Butia capitata* embryos (A) and water contents (dry basis) of seeds and embryos (B) under dehydrated (seeds with water contents of 5.4% on a fresh basis) or hydrated (seeds with water contents of 25.6% on a fresh basis) conditions. Different letters indicate that the treatments statistically differed from each other (Tukey test, $p < 0.05$). The bars represent the standard errors of the means.

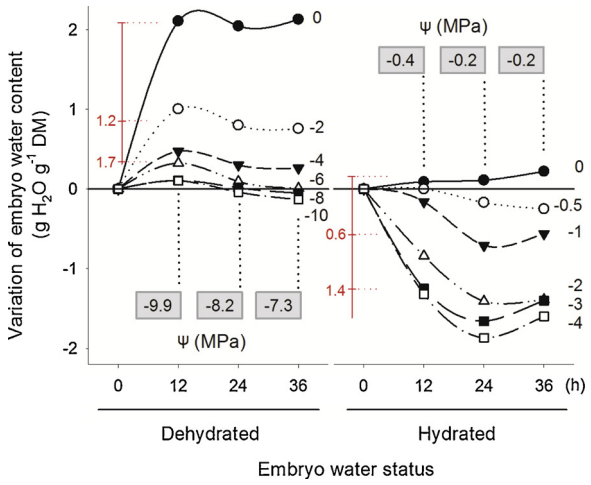

Fig. 2. Variation of the water contents (g H_2O g^{-1} DM) and ψ_w (MPa) of dehydrated (0.11 g H_2O g^{-1} DM) and hydrated (1.84 g H_2O g^{-1} DM) *Butia capitata* embryos after immersion in osmotic solutions with different ψ_w, during 36 h. The numbers at the end of the curves indicate the ψ_w (MPa) used in the treatments. The reductions of water capacity (the ability to absorb or retain water) in the treatments selected for the physiological evaluations are indicated in red. The numbers in the boxes indicate the ψ_w of the embryos at each time. (For interpretation of the references to colour in this figure legend, the reader is referred to the web version of this article.)

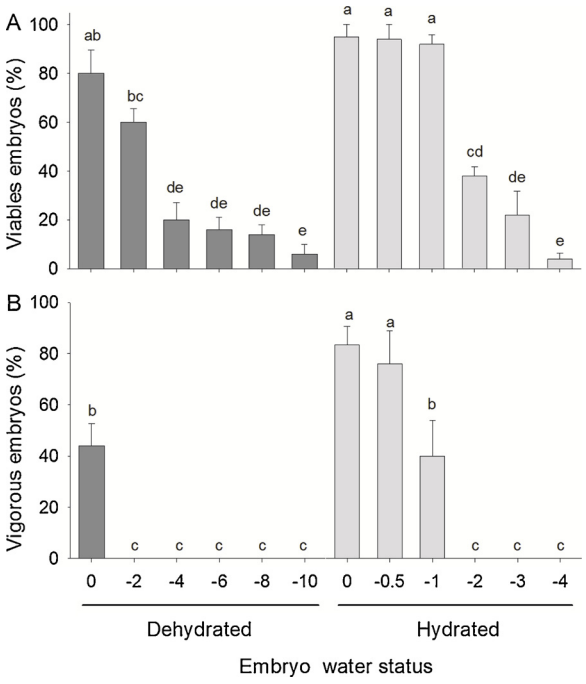

Fig. 3. Percentages of viable (A) and vigorous (B) *Butia capitata* embryos after immersion in osmotic solutions with different ψ_w for 12 h in dehydrated (0.11 g H_2O g^{-1} DM) or hydrated (1.84 g H_2O g^{-1} DM) conditions as evaluated by the tetrazolium test. Different letters indicate that the treatments statistically differed from each other (Tukey test, $p < 0.05$). The bars represent the standard errors of the means.

$\psi_w = 0$ MPa (Fig. 2). Increasing water contents were also noted in the other treatments in the first 12 h, with intensities influenced by the ψ_w of the solution. Water contents decreased at 24 h only under $\psi_w = -10$ MPa, and at 36 h under $\psi_w = -8$ and $\psi_w = -10$ MPa. In the case of the hydrated embryos (1.84 g H_2O g^{-1} DM), only $\psi_w = 0$ MPa caused an increase in their water contents. The intensities of the reductions of water contents under other treatments became more intense as ψ_w decreased.

The ψ_{ws} tested provided approximately two-fold variations in water capacities (defined here as the ability to absorb or retain water) of both dehydrated and hydrated embryos (Fig. 2). The ψ_w of the dehydrated embryos increased 26% after between 12 and 36 h of immersion in the solutions, with a mean of -8.5 MPa. Hydration promoted a 98% increase in ψ_w of the embryos, which stabilized at -0.2 MPa after 24 h of immersion in the osmotic solutions.

3.2. Viability and vigor

The variabilities of the dehydrated and hydrated embryos were 80 and 95% respectively, under initial condition, and were not significantly affected by immersion in distilled water ($\psi_w = 0$ MPa) for 12 h. Viability decreased with ψ_{ws} more negative than -2 and -1 MPa, with dehydrated or hydrated embryos respectively (Fig. 3A).

Hydrated embryos showed greater vigor in relation to dehydrated embryos when submitted to $\psi_w = 0$ MPa (Fig. 3B). That fact is related to the greater metabolic activity in hydrated embryos, considering that the tetrazolium test evaluates respiratory activity. It was observed that $\psi_w = -1$ MPa reduced the vigor of the hydrated embryos, and vigorous embryos were not identified when $\psi_{ws} \leq -2$ MPa with either hydrated or dehydrated embryos.

For the evaluations described in the following sections, in addition to the initial condition (control) and $\psi_w = 0$ MPa, treatments were chosen with ψ_{ws} that provided moderate and severe stress in dehydrated or hydrated embryos. For dehydrated embryos, $\psi_w = -2$ MPa was considered to induce moderate stress, since it reduced the water capacity (capacity to absorb or retain water in relation to $\psi_w = 0$) by 1.2 mg H_2O mg^{-1} DM (Fig. 2), did not significantly reduce embryo viability, and eliminated embryo vigor (Fig. 3A–B); $\psi_w = -4$ MPa was considered a severe stress inducer, as it reduced water capacity by 1.7 g H_2O g^{-1} DM (Fig. 2) and reduced embryo viability by 75% (Fig. 3A). For hydrated embryos, $\psi_w = -1$ MPa was considered a moderate stress inducer as it reduced water capacity by 0.6 g H_2O g^{-1} DM (Fig. 2), did not reduce viability, and decreased embryo vigor by 54% (Fig. 3A–B); $\psi_w = -2$ MPa was considered a severe stress inducer as it reduced water capacity by 1.4 g H_2O g^{-1} DM (Fig. 2), reduced embryo viability by more than 60%, and eliminated their vigor (Fig. 3A-B). Additionally, the effect of FH could be evaluated by comparing the effects of the exposure of dehydrated embryos directly to that of distilled water ($\psi_w = 0$ MPa), while the effects of slow hydration (SH) were evaluated by comparing the initial condition (controls) under dehydrated and hydrated conditions, as in that case, hydration was carried out over 72 h with the embryos still contained within the seeds.

3.3. Evaluation of ROS – histolocalization of O_2^- and quantification of H_2O_2

The embryos of *B. capitata* have two morphologically distinct regions: the cotyledonary petiole, which holds the embryonic axis (and plays a determinant role in germination), and the haustorium (Fig. 4), a region responsible for the mobilization of endospermic reserves (Oliveira et al., 2013; Dias et al., 2017).

In general, O_2^- production was significantly higher in hydrated embryos than in dehydrated embryos (Fig. 4). In the initial condition of dehydrated embryos, O_2^- was observed to accumulate at the apex of the cotyledonary petiole and throughout the haustorium. FH led to the expressive removal of O_2^- throughout the embryo, while SH caused intensification of O_2^- ion production in the same regions observed under initial conditions. Moderate stress ($\psi_w = -2$ MPa) of dehydrated embryos caused O_2^- production, especially in the cotyledonary petiole; severe stress ($\psi_w = -4$ MPa) caused O_2^- production at the apex of the cotyledonary petiole and throughout the haustorium. In hydrated embryos, exposure to both $\psi_w = 0$ and moderate stress ($\psi_w = -1$ MPa) led

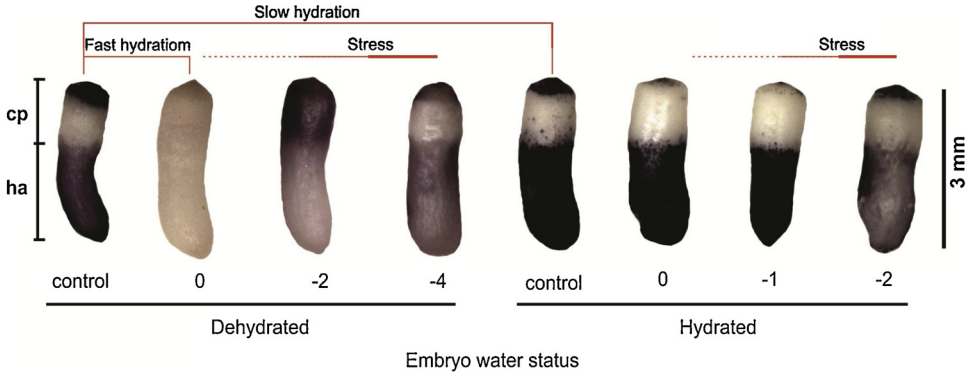

Fig. 4. Images of *Butia capitata* embryos after immersion in osmotic solutions with different ψ_w in dehydrated (0.11 g H_2O g^{-1} DM) or hydrated (1.84 g H_2O g^{-1} DM) conditions, stained with NBT for the histolocalization of O_2^- (identified by its purple color). The red lines indicate the main comparisons between the treatments that were highlighted in the text. cp: cotyledonary petiole; ha: haustorium. (For interpretation of the references to colour in this figure legend, the reader is referred to the web version of this article.)

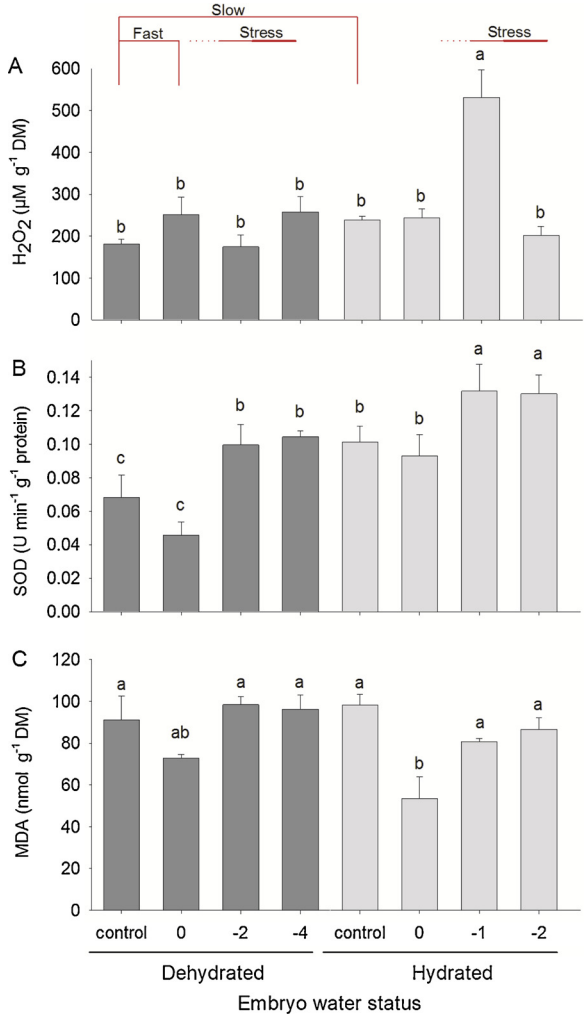

Fig. 5. H_2O_2 contents (A), SOD activities (B), and MDA contents (C) of *Butia capitata* embryos after immersion in osmotic solutions with different ψ_w under dehydrated (0.11 g H_2O g^{-1} DM) or hydrated (1.84 g H_2O g^{-1} DM) conditions. The red lines indicate the main comparisons between the treatments that were highlighted in the text. Fast: fast hydration; Slow: slow hydration. Different letters indicate that the treatments statistically differed from each other (Tukey test, $p < 0.05$). The bars represent the standard errors of the means. (For interpretation of the references to colour in this figure legend, the reader is referred to the web version of this article.)

to the removal of O_2^- from the cotyledonary petiole but its intense production in the haustorium; under severe stress (ψ_w = -2 MPa), O_2^- production became reduced in a pattern similar to that observed in dehydrated embryos under an identical level of stress.

H_2O_2 concentrations were not affected by FH or SH (Fig. 5A). Moderate and severe stress did not affect H_2O_2 concentrations in dehydrated embryos, while significant increases in H_2O_2 concentrations were observed in hydrated embryos only under moderate stress.

3.4. Antioxidant system enzyme activities and estimates of lipid peroxidation (MDA quantification)

No APX activity was detected, and there were no significant differences in CAT activities (M = 10.44 mmol min^{-1} g^{-1} protein; P = 0.407) among the treatments evaluated. FH did not affect SOD activity, although its activity increased with SH (Fig. 5B). Conditions of moderate and severe stress increased SOD activity in both dehydrated and dehydrated embryos. The lipid peroxidation indicator (MDA) was not affected by hydration or by the stresses to which the embryos were submitted (Fig. 5C), although exposure of hydrated embryos to ψ_w = 0 MPa reduced MDA concentrations in relation to other treatments.

3.5. ABA quantification

Both FH and SH significantly increased embryo ABA concentrations (Fig. 6). Moderate and severe stresses led dehydrated embryos to reduce their ABA contents, in relation to ψ_w = 0 MPa, although hormone levels remained higher than in the initial condition. Hydrated embryos

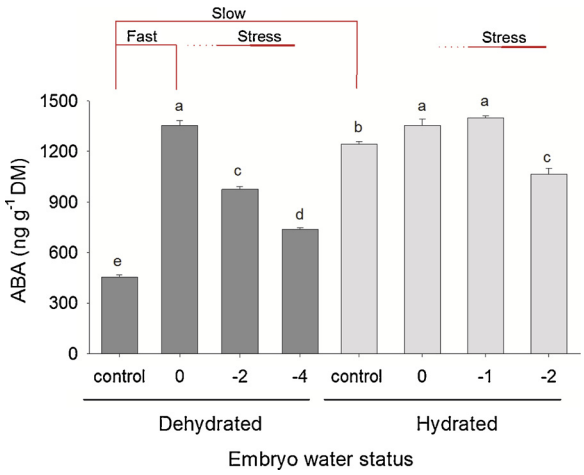

Fig. 6. ABA contents of *Butia capitata* embryos after immersion in osmotic solutions with different ψ_w in dehydrated (0.11 g H_2O g^{-1} DM) or hydrated (1.84 g H_2O g^{-1} DM) conditions. The red lines indicate the main comparisons between the treatments that were highlighted in the text. Fast: fast hydration; Slow: slow hydration. Different letters indicate that the treatments differed statistically from each other (Tukey test, $p < 0.05$). The bars represent the standard errors of the means. (For interpretation of the references to colour in this figure legend, the reader is referred to the web version of this article.)

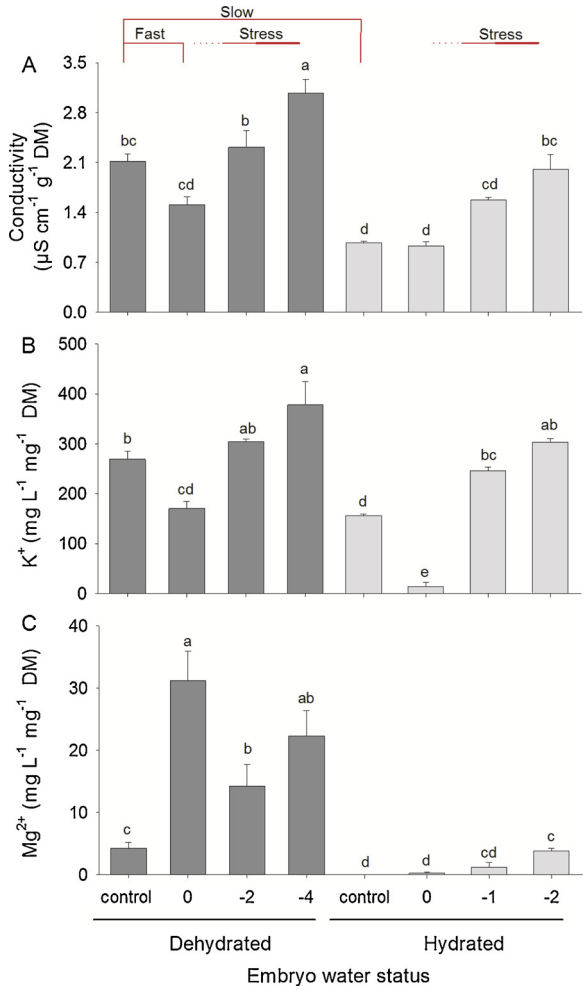

Fig. 7. Electrical conductivity (A), and leaching of K^+ (B) and Mg^{2+} (C) ions of *Butia capitata* embryos after immersion in osmotic solutions with different ψ_w in dehydrated (0.11 g H_2O g^{-1} DM) or hydrated (1.84 g H_2O g^{-1} DM) conditions. The red lines indicate the main comparisons between the treatments that were highlighted in the text. Fast: fast hydration; Slow: slow hydration. Different letters indicate that the treatments statistically differed from each other (Tukey test, $p < 0.05$). The bars represent the standard errors of the means. (For interpretation of the references to colour in this figure legend, the reader is referred to the web version of this article.)

exposed to $\psi_w = 0$ MPa, and to moderate stress, increased their ABA concentrations in relation to controls, while severe stress promoted a reduction in hormone content.

3.6. Cell membrane functionality – electrical conductivity and solute leaching

Dehydrated embryos generally showed low solute leaching control, resulting in higher levels of electrical conductivity and leached K^+ and Mg^{2+} (Fig. 7A–C). Evaluations of electrical conductivity and K^+ quantification presented very similar results, suggesting it to be the most leached ion. No effects of the treatments were observed on Ca^{2+} concentrations, however, indicating that the embryos retain that ion more tightly. Mg^{2+} leaching occurred at levels approximately 10 times less than those of K^+.

FH did not affect electrical conductivity, and led to reductions of K^+ leaching, although with increased Mg^{2+} leaching (Fig. 7A–C). SH improved the functionality of membranes with reduction in electrical conductivity and ion leaching. Moderate stress did not affected electrical conductivity or K^+ leaching in dehydrated embryos, although those characteristics were positively affected by severe stress (Fig. 7A–B). Mg^{2+} leaching increased in relation to controls under both moderate and severe stress (Fig. 7C). The exposure of hydrated embryos to $\psi_w = 0$ MPa for 12 h reduced K^+ leaching relative to controls, but did not affect conductivity or Mg^{2+} leaching (Fig. 7A–C). Moderate stress increased only K^+ leaching, while severe stress increased both the conductivity and leaching of both K^+ and Mg^{2+}.

3.7. Ultrastructural evaluations

The protoderm cells of the cotyledonary petiole, in their initial states, had thin and slightly sinuous walls; the cytoplasm was dense and rich in organelles, especially mitochondria, with dictyosomes and proplastids (Fig. 8A–B). Numerous small vacuoles showed stored proteins, as revealed by histochemical tests (data not shown). Hydrated embryos ($\psi_w = 0$ MPa) showed turgid cells with no wall sinuosities (Fig. 8C), with dense cytoplasm but reduced numbers of mitochondria and dictyosomes; endoplasmic reticulum proliferation, commonly associated with ribosomes, was observed (Fig. 8C–D). Fusions of vacuoles containing protein residues with flocculated appearances were also observed, indicating the beginning of reserve mobilization; numerous lipid bodies, identified by histochemical tests (data not shown), were organized around the vacuoles.

The immersion of the embryos in solutions with $\psi_w = -1$ MPa did not cause apparent damage to the protoderm cells (Fig. 8E–F). Protein reserves were more abundant inside the vacuoles as compared to the treatment $\psi_w = 0$ MPa, indicating some mobilization restrictions. Vacuoles commonly showed membrane residues in their interior. Glyoxysomes with granular matrices were observed in the cytoplasm, usually close to mitochondria and lipid bodies (Fig. 8F). The stress generated by immersion of embryos in solutions with $\psi_w = -2$ MPa resulted in severe damage to the protoderm cells. The cell walls showed accentuated sinuosities, and the protoplast was strongly retracted (Fig. 8G). There was a notable accumulation of substances in the periplasmic space, including lipids and membrane residues. The cytoplasm was not at all dense, with low populations of organelles, and without mitochondria, endoplasmic reticulum, dictyosomes, glyoxysomes, or plastids. Proteins remained accumulated in vacuoles, indicating restricted mobilization (Fig. 8H). Lipid bodies were randomly distributed in the cytoplasm, and many were partially degraded. Nuclei were observed at the cell periphery, being strongly contracted and without their nuclear envelopes (Fig. 8G).

The cells of the ground meristem of the cotyledonary petiole exhibited significant differences in relation to those of the protoderm. In the initial condition, proteins (evidenced by histochemical tests - data not shown) were stored in vacuoles of variable sizes distributed throughout the cytoplasm (Fig. 9A–B). Lipid bodies, with irregular contours, were positioned peripherally, and there were small starch grains in the cytoplasm. Embryo hydration resulted in intense protein mobilization and the formation of large vacuoles containing protein residues and flanked by small lipid bodies with circular contours (Fig. 9C–D).

Embryos exposed to $\psi_w = -1$ MPa also showed evidence of intense protein mobilization (unlike protoderm cells under the same conditions) (Fig. 9E), in addition to the presence of glyoxysomes, commonly associated with mitochondria (Fig. 9F). Under WS ($\psi_w = -2$ MPa), the cells appeared partially collapsed, with conspicuous wall invaginations (Fig. 9G–H). The proteins had not been mobilized and were observed in the cytoplasm and inside vacuoles (those also often with lipid bodies and membrane residues).

The main cytological changes seen in embryos in response to ψ_w are summarized in Fig. 10.

4. Discussion

The diaspore of the palm *B. capitata* is the pyrene (the seed enclosed

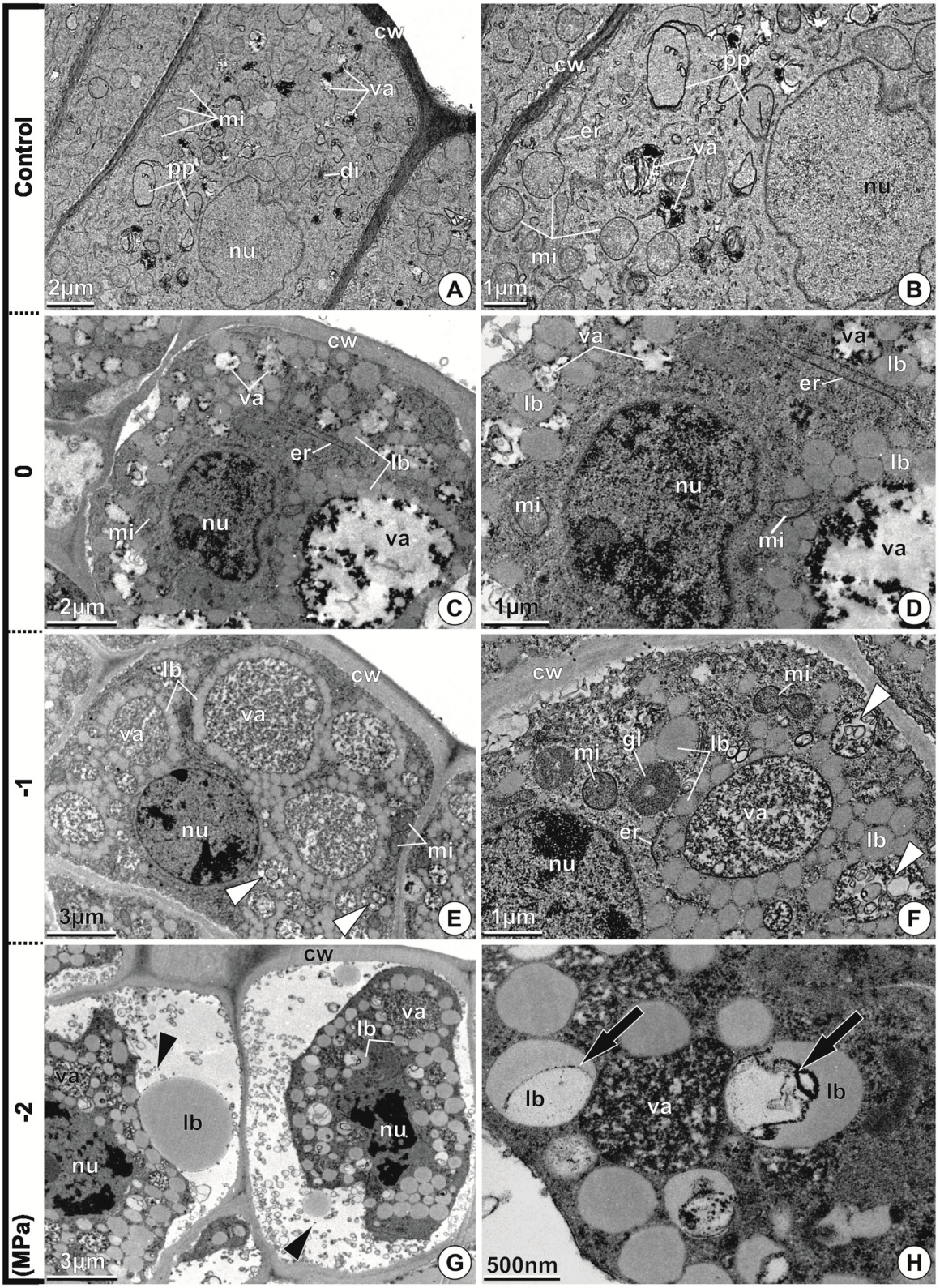

Fig. 8. Ultrastructure of the protoderm of *Butia capitata* embryos in dehydrated (0.11 g H_2O g^{-1} DM) (control) or hydrated (1.84 g H_2O g^{-1} DM) conditions and exposed to osmotic solutions with different ψ_w (indicated in the left column). A, B) Cell with thin walls; dense cytoplasm, rich in organelles, containing small protein vacuoles. C, D) Median region of the cell showing vacuoles containing protein residues, indicating the initiation of protein mobilization during imbibition. E) Cell containing protein vacuoles flanked by lipid bodies with circular outlines. F) Cell periphery, highlighting glyoxysomes, and membrane residues (white arrowheads) within protein vacuoles. G) Cell with notable contraction of the protoplast and accumulations of substances in the periplasmic space (black arrowheads); contracted nucleus without its nuclear membrane. H) Periphery of the cell, showing intense lipid mobilization (black arrows) and intact protein vacuoles. cw, cell wall; di, dictyosome; er, endoplasmic reticulum; gl, glyoxysome; lb, lipid bodies; mi, mitochondria; nu, nucleus; pp, proplastid; va, protein vacuole.

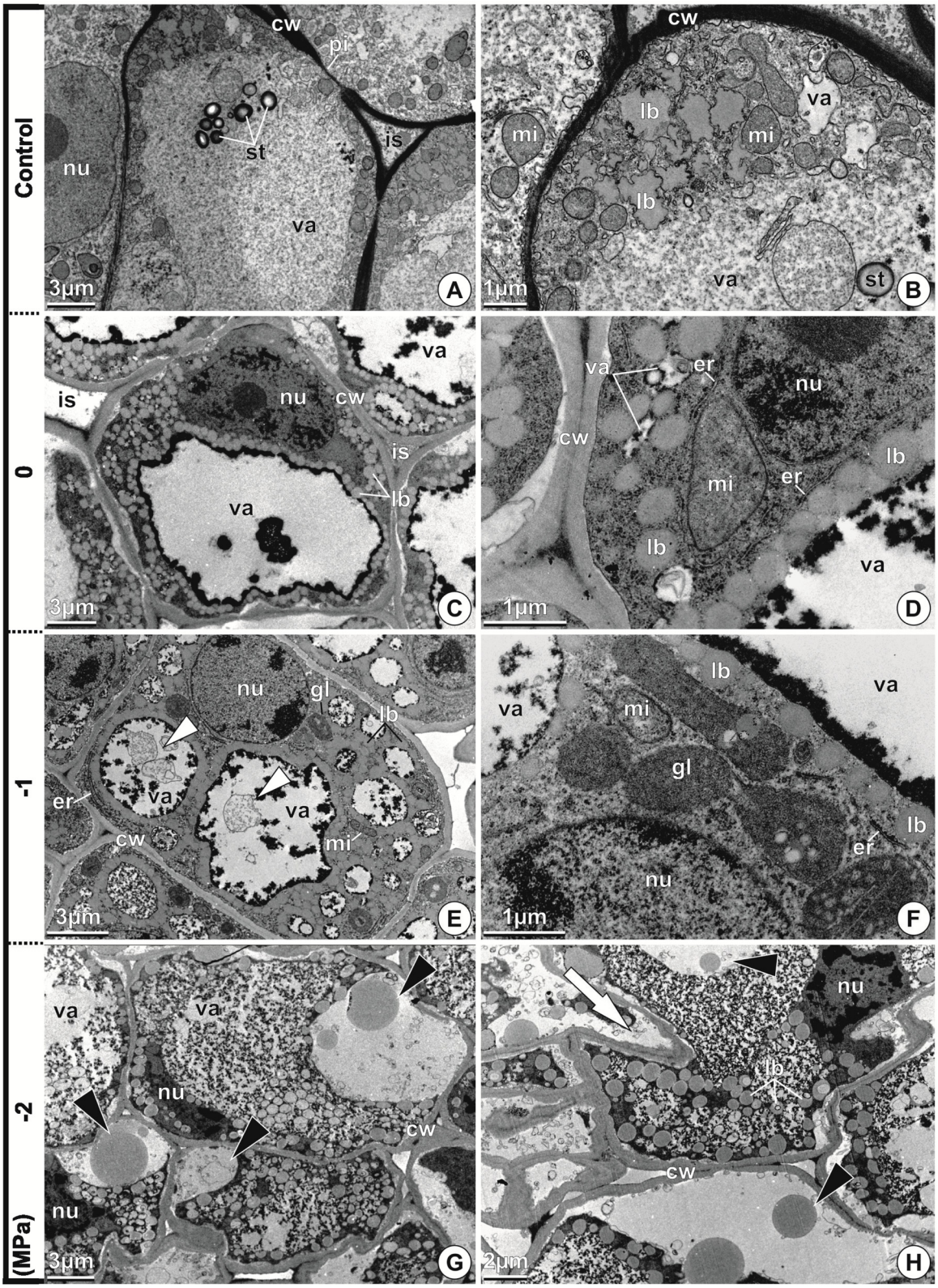

Fig. 9. Ultrastructure of the ground meristem of *Butia capitata* embryos in dehydrated (0.11 g H_2O g^{-1} DM) (control) or hydrated (1.84 g H_2O g^{-1} DM) conditions after immersion in osmotic solutions with different ψ_w (indicated in the left-hand column). A, B) Cells with thin walls, dense cytoplasm, rich in mitochondria, large protein vacuoles, lipid bodies, and starch. C, D) Cells with vacuoles containing protein residues with flocculated appearances, flanked by small lipid bodies with circular outlines. E) Cell with vacuoles containing proteins and membrane residues (white arrowheads). F) Cell periphery showing glyoxysomes associated with mitochondria and lipid bodies. G, H) Cell with strongly sinuous wall (white arrow), conspicuous contraction of protoplast, and accumulation of substances in the periplasmic space (black arrowheads); protein in vacuoles and in the cytoplasm. cw, cell wall; di, dictyosome; er, endoplasmic reticulum; gl, glyoxysome; is, intercellular space; lb, lipid bodies; mi, mitochondria; nu, nucleus; pi, primary pit field; pp, proplastid; st, starch; va, protein vacuole.

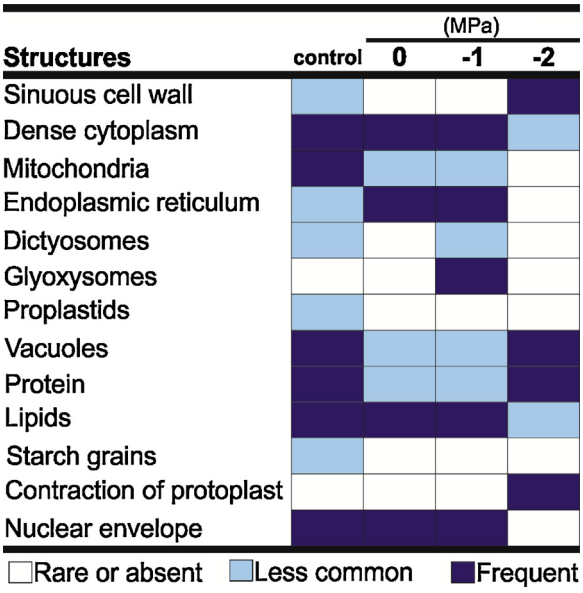

Fig. 10. Scheme illustrating changes in the cytological characteristics of *Butia capitata* embryos exposed to osmotic solutions with different ψ_w.

by the endocarp), which is normally incorporated into the soil seed bank after the fleshy mesocarp is consumed by dispersers (Oliveira et al., 2013). The endocarp is rigid and protects the seed, although the embryo maintains contact with the surrounding environment through the germinative pore, which provides a pathway for the flow of water and gas exchange (Fig. 11). Seeds can remain for long periods of time in seed banks due to their high levels of dormancy and so undergo repeated hydration cycles (Oliveira et al., 2013; Dias et al., 2015, 2017). We have shown here, through physiological and cytological evaluations, that the embryos of *B. capitata* are tolerant to extreme water events, which contributes to the resilience of their seed banks.

4.1. Aspects of WS tolerance

The embryos in *B. capitata* show high resistance to WS due to their water capacity, associated with abundant reserves, oxidative stress control, and high ABA contents. We observed that air dehydrated embryos (0.1 g H_2O g^{-1} DM) had low ψ_w (-8.5 MPa) and high water capacities (Fig. 2). Even the WS induced by ψ_w = -2 MPa, which normally does not occur in the soil (Kirkham, 2005) (but may occur after fires), did not affect the viability of the embryos due to the abundance of embryonic reserves (especially proteins and starch - Fig. 9A–B) already evidenced in other studies (Magalhães et al., 2013; Oliveira et al., 2013). Protein and amylaceous reserves directly influence the ψ_w matric, the main component of ψ_w related to the water capacity of dehydrated seeds (Nonogaki et al., 2010; Bewley et al., 2013). Additionally, numerous proteins and carbohydrates play crucial roles in protecting cell membranes under conditions of intense dehydration (Berjak and Pammenter, 2008; Marques et al., 2018). The preservative capacities of cell membranes are reflected in the low levels of solute leaching observed in (dehydrated or hydrated) *B. capitata* embryos when submitted to moderate stress (Fig. 11).

The ability to control oxidative stress in *B. capitata* embryos is associated with SOD activity (that was observed with moderate or severe stress in dehydrated or hydrated embryos), which probably contributed to controlling O_2^- levels (Fig. 11). Increased production of H_2O_2 was observed, on the other hand, in hydrated embryos submitted to moderate stress related to the proliferation of glyoxysomes (Fig. 9F), organelles involved in the production of H_2O_2 by the beta oxidation of lipids (Bailly, 2004; El-Maarouf-Bouteau and Bailly, 2008). Although high levels of H_2O_2 are commonly related to cell damage (Bailly, 2004; Diaz-Vivancos et al., 2013), we found that lipid peroxidation, membrane functionality, and cell structure were not affected by H_2O_2 production (Fig. 11). As the enzymatic antioxidant systems related to H_2O_2 scavenging (CAT and APX activity) were not activated, it is possible that alternative mechanisms of protection against oxidative stress are effective. Studies have shown that embryos of species phylogenetically related to *B. capitata* (Cocoseae tribe) accumulate the potent antioxidants tocopherols and tocotrienols (Siles et al., 2013; Barreto et al., 2014). Other studies have shown that oxidized forms of proteins play prominent roles in ROS scavenging (Job et al., 2005; Barba-Espín et al., 2012). The elucidation of the composition of the abundant protein reserves evidenced in *B. capitata* embryos (Oliveira et al., 2013), as well as additional research on non-enzymatic antioxidant mechanisms, will contribute to our knowledge of oxidative stress tolerance in that species.

Also worth noting were the high ABA contents observed in *B.*

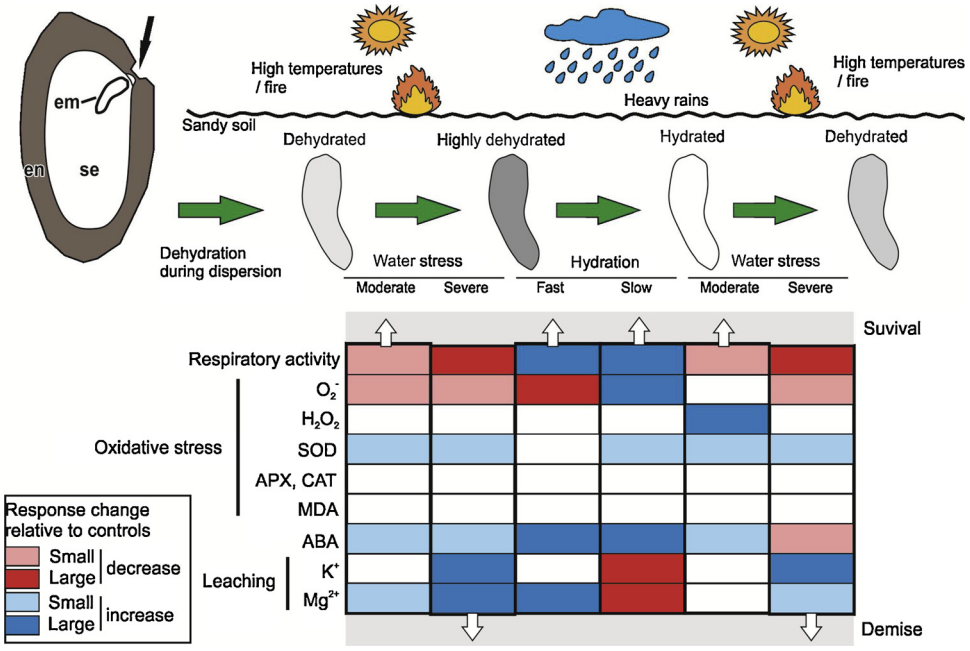

Fig. 11. Schematic illustration of the *Butia capitata* pyrene (upper left corner), with emphasis on the germinative pore (arrow), the main causes of water stress to which embryos in seed banks are submitted, and their associated physiological responses. The red and blue colors in the table indicate, respectively, decreases or increases of their responses in relation to controls (dehydrated or hydrated embryos in their initial conditions). Darker shades indicate greater response intensities. em, embryo; en, endocarp; se, seed. (For interpretation of the references to colour in this figure legend, the reader is referred to the web version of this article.)

capitata embryos together with its synthesis even with low metabolic rates (Fig. 11). High ABA concentrations were also observed in embryos of *Acrocomia aculeta* (Ribeiro et al., 2015) and *Attalea vitrivir* (Dias et al., 2017), palm trees with seeds that are highly tolerant to desiccation and also occur in the Cerrado biome. ABA is considered a key hormone in terms of tolerance to water stress, a condition that commonly promotes its increased biosynthesis (Ozfidan et al., 2012). That hormone acts as a messenger in several cellular signaling networks, and triggers the expression of genes related to stress tolerance and the activation of antioxidant systems, resulting in ROS reductions (Ozfidan et al., 2012; Souza et al., 2017). ABA synthesis, even under conditions of severe water stress, as evidenced in the present work, can be considered a key aspect of the desiccation tolerance of *B. capitata* embryos.

When severe WS ($\psi w = -2$ MPa) was applied, the hydrated embryos completely lost vigor and showed a 56% decline in viability – associated with a significant increase in ion leaching (Fig. 11). Under those conditions, there was also a blockage of protein mobilization, the collapse of cell structure (evidenced by the invagination of cell walls), reductions of organelle populations, protoplast retraction, the presence of residues and membranes in the periplasmic space, the loss of the nuclear envelope, and the degradation of lipids (Fig. 10). Together, those processes are common to WS responses due to biophysical damage to cellular components (Berjak and Pammenter, 2008).

4.2. Hydration effects on embryo physiology and ultrastructure

B. capitata embryos tolerate FH, and SH is associated with reserve mobilization, membrane functionality restoration, and oxidative stress control. Hydration is the first stage of the germination process, although FH is known to cause severe cellular damage in the seeds of several species (Bewley et al., 2013). Despite the considerable elevation of ψ_w, FH did not affect embryo viability (Fig. 11). Although FH promoted increased respiratory activity in *B. capitata* embryos, there was a reduction in O_2^- production; H_2O_2 production was not affected, however, suggesting that embryo metabolism was still adjusting to hydrated condition. With SH there was intense protein and starch mobilization (Figs. 8C–D; 9 C–D), which was related to increased respiratory activity and oxygen production. However the cellular protection mechanisms proved to be efficient. While SOD activity contributed to control oxidative stress, the restoration of membrane functionality resulted in expressive reductions of solute leaching in relation to the dehydrated condition (Fig. 11).

Seed imbibition is generally related to preparations for germinative processes involving resuming metabolic levels and the removal of inhibitors (Finch-Savage and Leubner-Metzger, 2006; Bewley et al., 2013). In the present work, however, we showed that ABA concentrations (one of the main inhibitors of germination) increased with embryo imbibition (Fig. 11). ABA synthesis by embryos is recognized as a mechanism for maintaining dormancy in the seeds of many species (Bewley et al., 2013), and the hormone is considered critical to controlling the germination of *B. capitata* and other Cerrado palm trees (Ribeiro et al., 2015; Dias et al., 2017). We consider the rapid synthesis of ABA in response to the hydration by embryos of *B. capitata* as constituting a mechanism to prevent germination under unstable environmental conditions such as those produced, for example, by the sparse rains typical of the Cerrado spring.

4.3. Insights into the persistence of Cerrado seed banks

B. capitata endemic to the Cerrado biome in central Brazil that are characterized by sandy soils and seasonal rainfall (Carvalho et al., 2015). The Cerrado is also prone to fires, which can contribute to extremely low soil ψ_w levels (Fichino et al., 2016). Dormancy is common in seeds of several Cerrado species (including about 50 palm species), leading to the formation of abundant and diverse seed banks (Lorenzi et al., 2010; Escobar et al., 2018; Souza et al., 2019). However, little is known about the physiological responses of tropical seeds to extreme water events. From the results of the present work, we are led to think that the association between an efficient antioxidant system and ABA biosynthesis capacity by embryos may be important for the maintenance of seed banks of other Cerrado species, which may be taken as a working hypothesis in future studies.

4.4. Conclusions

The embryos of *B. capitata* have high resistance to WS due to their abundant reserves, mechanisms of oxidative stress control, and high ABA biosynthetic capacity. Embryos tolerate FH, and there is a re-establishment of membrane functionality and an increase in ABA production with SH. The loss of embryo viability under severe stress is due to biophysical damage to cell structures. The tolerance of *B. capitata* embryos to WS and FH is determinant for the resilience of its seed banks in environments under the seasonal climate of the Cerrado biome.

Author contribution statement

LMR and PSNL conceived the work. BGG performed the experiments, collected the samples, and drafted the initial text. DSD performed the analyses and interpreted the results of oxidative stress. CPSM performed the analyses and interpreted the ABA results. HCM-S and MOM-S performed the ultrastructural and cytochemical evaluations and interpreted the related results. LMR and PSNL interpreted data on water relations. LMR drafted the final text. All authors have read the final version of the manuscript and agreed to its submission.

Declaration of Competing Interest

The authors declare that they have no conflict of interest.

Acknowledgements

The authors would like to thank the Coordenação de Aperfeiçoamento de Pessoal de Nível Superior - CAPES, for granting a master's degree grant to BGG, the Conselho Nacional de Desenvolvimento Científico e Tecnológico - CNPq for the postdoctoral fellowship awarded to CPSM, and the research productivity grants granted to LMR, PSNL and MOM-S.

References

Alexieva, V., Sergiev, I., Mapelli, S., Karanov, E., 2001. The effect of drought and ultraviolet radiation on growth and stress markers in pea and wheat. Plant Cell Environ. 24, 1337–1344.
Apel, K., Hirt, H., 2004. Reactive oxygen species: metabolism, oxidative stress, and signal transduction. Annu. Rev. Plant Biol. 55, 373–399.
Bailly, C., 2004. Active oxygen species and antioxidants in seed biology. Seed Sci. Res. 14, 93–107.
Barba-Espín, G., Hernández, J.A., Diaz-Vivancos, P., 2012. Role of H_2O_2 in pea seed germination. Plant Signal. Behav. 7, 193–195.
Barreto, L.C., Garcia, Q.S., Morales, M., Müller, M., Munné-Bosch, S., 2014. Vitamin E and defense-related phytohormones are reliable markers of embryo growth in macaw palm fruits exposed to various storage conditions. Plant Cell Tissue Org. Cult. 118, 203–213.
Baskin, C.C., Baskin, J.M., 2014. Seeds: Ecology, Biogeography and Evolution of Dormancy and Germination. Academic Press, San Diego.
Berjak, P., Pammenter, N.W., 2008. From Avicennia to Zizania: seed recalcitrance in perspective. Ann. Bot. 101, 213–228.
Bewley, J.D., Bradford, K.J., Hilhorst, H.W.M., Nonogak, H. (Eds.), 2013. Seeds: Physiology of Development, Germination and Dormancy. Springer, New York.
Bicalho, E.M., Santos, T.R., Garcia, Q.S., 2019. Abscisic acid and the antioxidant system are involved in germination of *Butia capitata* seeds. Acta Bot. Bras. 33, 174–178.
Brasil, 2009. Regras para análise de sementes. Ministério da Agricultura, Pecuária e Abastecimento, Brasília, DF.
Cakmak, I., Horst, W.J., 1991. Effect of aluminium on lipid peroxidation, superoxide dismutase, catalase, and peroxidase activities in root tips of soybean (*Glycine max*). Physiol. Plant. 83, 463–468.
Carvalho, V.S., Ribeiro, L.M., Lopes, P.S.N., Agostinho, C.O., Matias, L.J., Mercadante-Simões, M.O., Correia, L.N.F., 2015. Dormancy is modulated by seed structures in

palms of the Cerrado biome. Aust. J. Bot. 63, 444–454.
Dias, D.S., Lopes, P.S.N., Ribeiro, L.M., Oliveira, L.A.A., Mendes, E.V., Carvalho, V.S., 2015. Tolerance of desiccation and cryopreservation of *Butia capitata* palm seeds. Seed Sci. Technol. 43, 90–100.
Dias, D.S., Ribeiro, L.M., Lopes, P.S.N., Munné-Bosch, S., Garcia, Q.S., 2017. Hormonal profile and the role of cell expansion in the germination control of Cerrado biome palm seeds. Plant Physiol. Biochem. 118, 168–177.
Diaz-Vivancos, P., Barba-Espín, G., Hernández, J.A., 2013. Elucidating hormonal/ROS networks during seed germination: insights and perspectives. Plant Cell Rep. 32, 1491–1502.
El-Maarouf-Bouteau, H., Bailly, C., 2008. Oxidative signaling in seed germination and dormancy. Plant Signal. Behav. 3, 175–182.
Escobar, D.F.E., Silveira, F.A.O., Morellato, L.P.C., 2018. Timing of seed dispersal and seed dormancy in Brazilian savanna: two solutions to face seasonality. Ann. Bot. 121, 1197–1209.
Feder, N., O'Brien, T.P., 1968. Plant microtechnique: some principles and new methods. Am. J. Bot. 55, 123–142.
Fichino, B.S., Dombroski, J.R., Pivello, V.R., Fidelis, A., 2016. Does fire trigger seed germination in the Neotropical Savannas? Experimental tests with six Cerrado species. Biotropica 48, 181–187.
Finch-Savage, W.E., Leubner-Metzger, G., 2006. Seed dormancy and the control of germination. New Phytol. 171, 501–523.
Giannopolitis, C.N., Ries, S.K., 1977. Superoxide dismutases. I. Occurrence in higher plants. Plant Phys. 59, 309–314.
Gomes-Copeland, K.K.P., Lédo, A.D.S., Almeida, F.T.C.D., Miranda, R.P., Santos, I.R.I., 2012. Assessing the viability of cryopreserved coconut zygotic embryos by electrolytic conductivity and potassium leaching. Pesq. Agrop. Bras. 47, 8–13.
Heath, R.L., Packer, L., 1968. Photoperoxidation in isolated chloroplasts: I. Kinetics and stoichiometry of fatty acid peroxidation. Arch. Biochem. Biophys. 125, 189–198.
Huang, H., Song, 2013. Change in desiccation tolerance of maize embryos during development and germination at different water potential PEG-6000 in relation to oxidative process. Plant Physiol. Biochem. 68, 61–70.
Job, C., Rajjou, L., Lovigny, Y., Belghazi, M., Job, D., 2005. Patterns of protein oxidation in Arabidopsis seeds and during germination. Plant Physiol. 138, 790–802.
Johansen, D.A., 1940. Plant Microtechnique. McGraw-Hill, New York.
Karnovsky, M.J.A., 1965. A formaldehyde-glutaraldehyde fixate of high osmolality for use in electron microscopy. J. Cell Biol. 27, 137A–138A.
Kirkham, M.B., 2005. Principles of Soil and Plant Water Relations. Elsevier Academic Press, Amsterdam; New York.
Long, R.L., Gorecki, M.J., Renton, M., Scott, J.K., Colville, L., Goggin, D.E., Commander, L.E., Westcott, D.A., Cherry, H., Finch-Savage, W.E., 2014. The ecophysiology of seed persistence: a mechanistic view of the journey to germination or demise. Biol. Rev. 90, 31–59.
Lorenzi, H., Noblick, L.R., Kahn, F., Ferreira, E., 2010. Brazilian Flora: Arecaceae (Palms). Instituto Plantarum, Nova Odessa.
Magalhães, H.M., Lopes, P.S.N., Ribeiro, L.M., Sant'Anna-Santos, B.F., Oliveira, D.M.T., 2013. Structure of the zygotic embryos and seedlings of *Butia capitata* (Arecaceae). Trees 27, 273–283.
Marques, A., Buijs, G., Ligterink, W., Hilhorst, H., 2018. Evolutionary ecophysiology of seed desiccation sensitivity. Funct. Plant Biol. 45, 1083–1095.
Mazzottini-dos-Santos, H.C., Ribeiro, L.M., Oliveira, D.M.T., 2018. Structural changes in the micropylar region and overcoming dormancy in Cerrado palms seeds. Trees 32, 1415–1428.
Michel, B.E., Kaufmann, M.R., 1973. The osmotic potential of polyethylene glycol 6000. Plant Physiol. 51, 914–916.
Müller, M.L., Munné-Bosch, S., 2011. Rapid and sensitive hormonal profiling of complex plant samples by liquid chromatography coupled to electrospray ionization tandem mass spectrometry. Plant Methods 7, 37.
Nakano, Y., Asada, K., 1981. Hydrogen peroxide is scavenged by ascorbate-specific peroxidase in spinach chloroplasts. Plant Cell Physiol. 22, 867–880.
Nonogaki, H., Bassel, G.W., Bewley, J.D., 2010. Germination—still a mystery. Plant Sci. 179, 574–581.
Oliveira, N.C.C., Lopes, P.S.N., Ribeiro, L.M., Mercandante-Simões, M.O., Oliveira, L.A.A., Silvério, F.O., 2013. Seed structure, germination, and reserve mobilization in *Butia capitata* (Arecaceae). Trees 27, 1633–1645.
Oracz, K., Voegele, A., Tarkowská, D., Jacquemoud, D., Turecková, V., Urbanová, T., Strnad, M., Sliwinska, E., Leubner-Metzger, G., 2012. Myrigalone A inhibits *Lepidium sativum* seed germination by interference with gibberellin metabolism and apoplastic superoxide production required for embryo extension growth and endosperm rupture. Plant Cell Physiol. 53, 81–95.
Ozfidan, C., Turkan, I., Sekmen, A.H., Seckin, B., 2012. Abscisic acid-regulated responses of aba2-1 under osmotic stress: the abscisic acid-inducible antioxidant defense system and reactive oxygen species production. Plant Biol. 14, 337–346.
Reynolds, E.S., 1963. The use of lead citrate at high pH as an electron-opaque stain in electron microscopy. J. Cell Biol. 17, 208–212.
Ribeiro, L.M., Garcia, Q.S., Müller, M., Munné-Bosch, S., 2015. Tissue specific hormonal profiling during dormancy release in macaw palm seeds. Physiol. Plant. 153, 627–642.
Ribeiro, L.M., Garcia, Q.S., Oliveira, D.M.T., Neves, S.C., 2010. Critérios para o teste de tetrazólio na estimativa do potencial germinativo em macaúba. Pesq. Agrop. Bras. 45, 361–368.
Roland, A.M., 1978. General preparations and staining of thin sections. In: Hall, J.L. (Ed.), Electron Microscopy and Cytochemistry of Plant Cells. Elsevier, New York.
Siles, L., Cela, J., Munné-Bosch, S., 2013. Vitamin E analyses in seeds reveal a dominant presence of tocotrienols over tocopherols in the Arecaceae family. Phytochemistry 95, 207–214.
Souza, L.A., Monteiro, C.C., Carvalho, R.F., Gratão, P.L., Azevedo, R.A., 2017. Dealing with abiotic stresses: an integrative view of how phytohormones control abiotic stress-induced oxidative stress. Theor. Exp. Plant Physiol. 29, 109–127.
Souza, J.N.e, Agostinho, C., de, O., Ribeiro, L.M., Azevedo, A.M., Lopes, P.S.N., 2019. Edaphic and climatic control of macaúba palm seed bank dynamics. Ind. Crop. Prod. 141, 111802.
Vidal, B.C., 1970. Dichroism in collagen bundles stained with Xylidine-Ponceau 2R. Ann. Histochim. 15, 289–296.
Watson, M.L., 1958. Staining of tissue sections for electron microscopy with heavy metals II. Application of solutions containing lead and barium. J. Biophysic. Biochem. Cxtol. 727–730.